

Introduction

Here, we design new ultralight carbon aerogels with analogic 'long span structures' by scalable assembling 1D multiwalled carbon nanotube (CNT) and 2D giant graphene sheets together. The giant size of skeleton-behaved graphene sheets endowed the carbon aerogels with ultralow density as low as 0.75 mg/cm³. The synergistic effect between graphene skeletons and CNT reinforcing ribs engender the assembled carbon aerogels perform excellent elasticity in a broad temperature range from -190 °C to 300 °C. The highly porous carbon aerogel also exhibited the record absorption efficiency for organic liquids, up to 657 times of its own weight. The integration of ultralow density and robust elasticity of scalably assembled carbon aerogel may be useful in sensors, flexible electronic devices and environmental protections.

Results

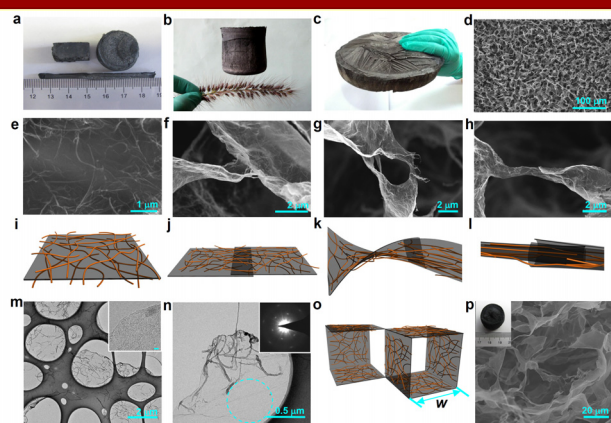


Figure 1. Macroscopic and Microscopic structures of UFAs. (a) Digital photograph of UFAs with diverse shapes. (b) A 100 cm³ UFA cylinder standing on a flower like dog's tail (*Setaira viridis* (L.) Beauv.). (c) A ~1000 cm³ UFA cylinder (21 cm in diameter and 3 cm in thickness). (d-e) Microscopically porous architecture of a UFA at different magnifications, showing CNT-coated graphene cell walls. (f-h) SEM images of different interconnections for CNTs-coated graphene (graphene@CNTs) cell walls: overlapping (f), twisting (g), and enveloping (h). (i) Cartoon of a flattened CNT-coated graphene cell wall. (j-l) Cartoon models corresponding to the three interconnection styles shown in (f-g) respectively. The gray lamellar, orange wires and brown wires represent the graphene sheet, CNTs coated on the top and CNTs coated on the back of the graphene sheet, respectively. (m,n) TEM images of CNT-coated graphene cell walls, the HRTEM image of a cell wall edge (inset in (m), scale bar is 2 nm) and the SAED patterns (inset in (n)) taken at the labeled area. (o) Schematic illustration of idealized building cells of our UFA made by synergistic assembly of graphene and CNTs. (p) SEM image and photograph (inset in (p)) of the lightest neat graphene aerogel ($\rho = 0.16$ mg cm⁻³, i.e. 1.38 mg in 8.6 cm³).

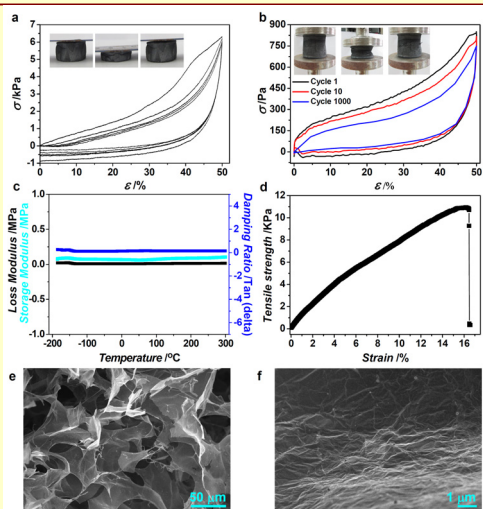


Figure 2. Viscoelastic properties of our UFA. (a) Stress-strain (σ - ϵ) curves of multicycle compressions on a UFA ($\rho = 5.6$ mg cm⁻³, $f = 0.5$), exhibiting recoverable deformation. (b) Stress-strain curves of several selected cycles on a UFA ($\rho = 1$ mg cm⁻³, $f = 0.5$) during repeated compression (the 1st, 10th and 100th cycle). (c) Temperature dependence of the storage modulus (cyan), loss modulus (black) and damping ratio (blue) of the UFA ($r = 7.6$ mg cm⁻³, $f = 0.5$). (d) Typical mechanical measurements under tensile loading of UFA ($r = 1.5$ mg cm⁻³, $f = 0.5$). The strain rate is 5 % min⁻¹. (e-f) SEM images of the UFA ($r = 1$ mg cm⁻³, $f = 0.5$) after 1000 cycles of compression-release process at different magnifications.

Results

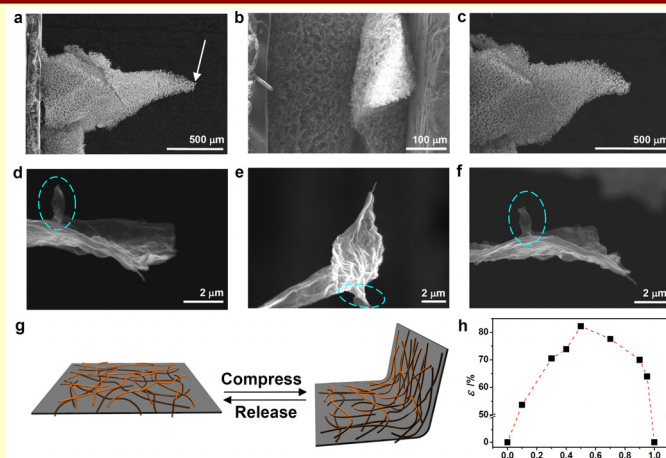


Figure 3. *In situ* SEM observations of UFAs under cycled compression. (a-c) The compression and release process of the UFA ($\rho = 2$ mg cm⁻³, $f = 0.5$). a, Before deformation. (b) Under deformation. (c) Full recovery after removal of load. (d-f) The recoverable deformation process of one single graphene@CNTs cell wall at the taper tip (indicated by the arrow in (a)). (d) Original shape. (e) Under deformation. (f) Full recovery after removal of load. The blue cycle indicates the frame of reference for SEM observations. (g) The schematic model of a single graphene@CNTs cell wall in the process of compressing and releasing shows the elastic mechanism of our UFAs: the deformation of cell walls rather than the sliding between them. (h) The recoverable compressive strain (ϵ) of the UFA ($\rho = 1.5$ mg cm⁻³) as a function of graphene weight fraction (f) in the UFA.

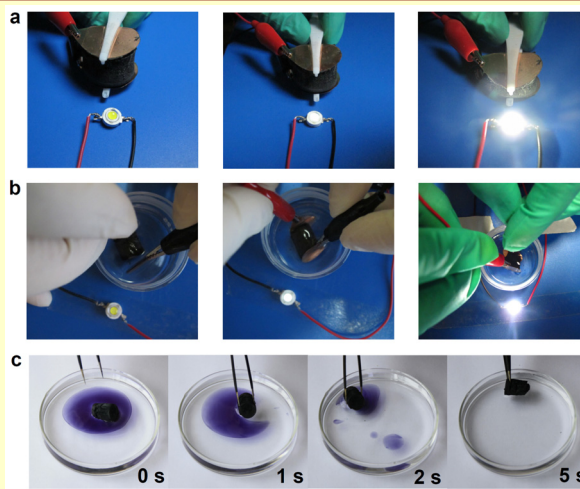


Figure 4. Elasticity-responsive conductivity and the oil absorption properties of the UFA ($r = 1.4$ mg cm⁻³, $f = 0.5$). (a) A circuit constructed with the UFA as lightweight conductive bulk. The brightness fluctuates upon compressing and releasing UFA. (b) The circuit constructed with the UFA ($\rho = 1.4$ mg cm⁻³, $f = 0.5$) as ultralight conductive bulk filled with n-hexane. The brightness fluctuates upon compressing and releasing UFA. (c) Absorption process of toluene (stained with Sudan Black B) on water by the UFA within 5 s.

Conclusions

In summary, we have developed a template-free, synergistic assembly strategy for the scalable fabrication of macroscopic, multimorph (1D, 2D and 3D), ultralight aerogels with controlled densities. The as-prepared aerogels are of outstanding temperature-invariant elasticity, ultralow density, excellent thermal stability, extremely high absorption capacities for organic liquids and PCMs, and good electrical conductivity.

Acknowledgements

This work was financially supported by the National Natural Science Foundation of China (No. 20974093 and No. 51173162), Qianjiang Talent Foundation of Zhejiang Province (No. 2010R10021), Fundamental Research Funds for the Central Universities (No. 2011QNA4029), Research Fund for the Doctoral Program of Higher Education of China (No. 20100101110049), and Zhejiang Provincial Natural Science Foundation of China (No. R4110175).